

## Acceleration and double-peak spectrum of hot electrons in relativistic laser plasmas

Shi-Bing Liu,<sup>1,2</sup> Jie Zhang,<sup>1</sup> and Wei Yu<sup>3</sup>

<sup>1</sup>Laboratory of Optical Physics, Institute of Physics, Chinese Academy of Sciences, P.O. Box 603, Beijing 100080, People's Republic of China

<sup>2</sup>CCAST (World Laboratory), P.O. Box 2735, Beijing 100080, People's Republic of China

<sup>3</sup>Shanghai Institute of Optics and Fine Mechanics, Chinese Academy of Sciences, P.O. Box 800-211, Shanghai 201800, People's Republic of China

(Received 15 June 1998; revised manuscript received 17 May 1999)

A spectrum equation of hot electrons in relativistic laser plasmas is derived in which two hot-electron population peaks appear as the laser strength parameter reaches a threshold. These calculations can explain the generation of very hot electrons with several tens of MeV energy and two hot-electron population peaks observed in the recent experiments. [S1063-651X(99)06009-2]

PACS number(s): 52.40.Nk, 42.55.Vc, 52.50.Jm, 34.80.Qb

In a recent experiment [1], very hot electrons with energy up to 20 MeV were observed and two hot-electron population peaks with different energies were characterized in the interaction of a high-intensity femtosecond laser pulse (1  $\mu\text{m}$ , 300 fs,  $10^{19}$  W/cm<sup>2</sup>) with an underdense plasma. This result was attributed to be due to the direct acceleration by the Lorentz force of the enhanced laser intensity in the channels formed by self-focus in the interaction. However, there is not a good theory to support their assumption. In this paper, we present a calculation based on relativistic Hamilton-Jacobi equation [2] to provide a theoretical explanation of the experimental result.

Considering the experimental circumstances in laser-solid target interactions, we assume that the initial electrons produced by prepulses, before the arrival of the main pulse, have initial momentum  $\mathbf{p}_0$  and energy  $\varepsilon_0$  and are in a Maxwellian distribution due to a long time delay (picosecond order) between the main pulse and the prepulse. During the main laser pulse (fs time scale) the ions can be treated as a rest plasma background in the process of interaction. The motion of electrons in the laser field can be described by the relativistic Hamilton-Jacobi equation [2]

$$[\partial_t S(\mathbf{r}, t) - (e/c)\mathbf{A}(\boldsymbol{\eta})]^2 - (1/c^2)[\partial_t S(\mathbf{r}, t)]^2 + m^2 c^2 = 0, \quad (1)$$

where  $S(\mathbf{r}, t)$  is the Hamilton principal function,  $\mathbf{A}(\boldsymbol{\eta})$  is the vector potential of laser field,  $\boldsymbol{\eta} = \omega_L t - \mathbf{k}_L \cdot \mathbf{r}$  is the Lorentz-invariant phase,  $(\omega_L, k_L = |\mathbf{k}_L|)$  are the frequency and wave number of the laser light, respectively, and  $m$  is the rest mass of the electron. For the case in which the electron is in rest ( $\mathbf{p}_0 = 0$ ) before interaction, Eq. (1) was already accurately solved [2]. In our case the motion of electrons produced by prepulse has to be taken into account.

We assume the laser pulse as a linearly polarized monochromatic plane wave with relativistic intensity and propagating along the  $z$  axis in the plasma produced by the prepulse. We choose the direction of the electric field of the laser in the  $x$  axis,  $\mathbf{E}_L = E_L \mathbf{e}_x \cos \eta$ . By a standard method the relativistic momentum equation of electrons quivering in a laser field can be found as

$$\mathbf{p}_E = -m v_E \mathbf{e}_x \cos \eta + \xi m v_E \mathbf{e}_z \cos \eta. \quad (2)$$

Correspondingly, the relativistic energy equation, due to the relativistic momentum-energy relationship  $\varepsilon = c(p^2 + m^2 c^2)^{1/2}$ , can be written as

$$\varepsilon(\mathbf{p}_E) = \xi m v_E c \cos \eta, \quad (3)$$

where

$$\xi = \frac{m v_E \cos \eta - 2 \mathbf{p}_0 \cdot \mathbf{e}_x}{2(\varepsilon_0/c - \mathbf{p}_0 \cdot \mathbf{e}_x)}. \quad (4)$$

In the above equations  $v_E = eE_L/(m\omega_L)$ ,  $\mathbf{e}_z$  is a unit vector in the laser propagation direction. In Eq. (2) the momentum of the electron includes two parts produced, respectively, by the laser electric field (transverse) and the Lorentz force of the laser magnetic field (longitudinal). From Eqs. (2)–(4) one can see that in the longitudinal component of the electron quiver momentum the initial motion of electrons produced by the prepulse is nonlinearly involved, as expected. The electrons in the preplasmas, due to the duration of the electron-electron process being shorter than the delay time between main pulse and prepulse, reach a thermal equilibrium within a short time period. When the laser pulse interacts with these electrons the electrons start to oscillate and acquire an acceleration along the laser propagation direction due to the zero-frequency part of  $E^2(\boldsymbol{\eta})$  at the leading edge of the pulse. Also, a harmonic would be produced due to the  $2\eta$  part of the laser field. In the transverse direction all harmonics are also contained due to the first term in Eq. (2). In the center of the pulse (reached its constant value) the electrons undergo various harmonic motions at a center of self-drifting. In principle, therefore, Eqs. (2) and (3) are enough to describe the motion of relativistic electrons produced by laser-plasma interaction in the presence of prepulses.

For a femtosecond time scale and high intensity laser pulse, the plasma heating mechanisms are not very important [3]. Because the initial electrons are in a Maxwellian distribution, by a general transformation of momentum and energy such a spectrum equation of electrons can be found by taking into account the experimental conditions

$$\frac{dN_e(\varepsilon_k, \eta)}{d\varepsilon_k} = A_0 \frac{(1 + 1.957\varepsilon_k)N_0}{\gamma_0 \sqrt{I\lambda^2}} \frac{\sinh[\psi_1(\eta)]}{(1 + \xi^2)^{1/2} \cos \eta} \times \exp[-\psi_2(\eta)], \quad (5)$$

where

$$\psi_1(\eta) = \frac{pp_E(\eta)}{\gamma_0^2 m^2 c^2}, \quad \psi_2(\eta) = \frac{p^2 + p_E^2(\eta)}{2\gamma_0^2 m^2 c^2}. \quad (6)$$

And here  $A_0 \approx 1.823 \times 10^9$  ( $\text{MeV}^{-1}$ ),  $p^2 = \varepsilon^2/c^2 - m^2 c^2$ ,  $\gamma_0 = p_0/(mc)$ ,  $\varepsilon_k = \varepsilon - mc^2$  is the kinetic energy of electron,  $N_0$  is the total number of ionized electrons,  $I(\lambda)$  is laser intensity (wavelength), and the units of  $I\lambda^2$  and  $\varepsilon_k$  are  $\text{W cm}^{-2} \mu\text{m}^2$  and  $\text{MeV}$ , respectively.  $dN_e/d\varepsilon_k$  is the number of electrons in a 1 MeV energy interval. In the above derivations we neglected the heating effects of forward-Raman-scattering (FRS) instability and plasma instabilities, and our reasons are based on the following facts. In underdense plasmas, because electrons are expelled from the focal spot by the ponderomotive pressure of intense laser pulses, a plasma channel [4] is formed, which was also observed in experiments [1]. A two-dimensional (2D) particle-in-cell (PIC) simulation [5] shows that at very high laser intensities the electrons can be strongly heated even in the absence of FRS instability, which implies that FRS instability in the formed channel may not play a significant role for the generation of very hot electrons. Another analytical theory and 2D PIC simulations [6] show also that in hollow channel plasmas the FRS instability would completely destroy the beam in homogeneous plasmas or parabolic channel plasmas at very high laser intensities. However, this instability in the formed channel can be completely suppressed. For some plasma instabilities [7], the ponderomotive force acts always to prevent the growth of excited plasma waves from instabilities due to  $\omega_L \gg \omega_p$  (where  $\omega_p$  is the frequency of the plasma).

For applications it is useful to average the spectrum equation (5) over the phase of the laser field. First we consider an averaging effect of coupling between the initial motion and the longitudinal motion of electrons. We find from numerical calculations that when the laser strength parameter (LSP) of the laser pulse exceeds the threshold  $(I\lambda^2)_{\text{th}} \geq 5.5 \times 10^{18} \text{ W cm}^{-2} \mu\text{m}^2$  the second hot-electron peak appears at initial velocity  $v_0 = 0.1c$  ( $\sim 2.5$  keV). This threshold agrees well with the experimental result ( $\geq 5.0 \times 10^{18} \text{ W cm}^{-2} \mu\text{m}^2$ ) [1]. Using the laser parameters in the experiment, the calculated hot-electron spectrum vs electron kinetic energy is plotted in Fig. 1. It is interesting to note that, for an initial velocity  $v_0 = 0.2c$ , the hot-electron population peaks at two energies of 1.7 and 3.4 MeV, respectively, and when the intensity of laser pulse is increased to  $2 \times 10^{19} \text{ W cm}^{-2}$  and  $v_0 = 0.3c$  these two peaks are moved to 4.2 and 6.7 MeV, respectively. It is interesting to find that by using the enhanced laser intensity ( $10^{20} \text{ W/cm}^2$ ) in the channel [8] the energy for the second hot-electron peak can exceed 20 MeV for the initial electrons moving in the direction of laser propagation, which agrees well with the experimental observation [1]. We can also find from Fig. 1 that the energy corresponding to the first hot-electron peak does not vary with the change of the initial velocity but that corre-

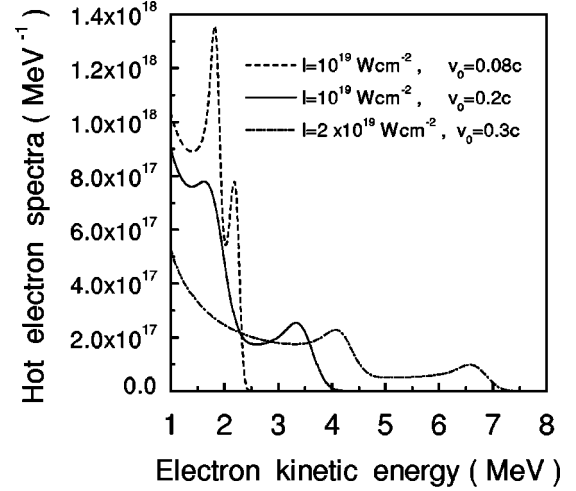


FIG. 1. With laser parameters the same as used in the experiment ( $I = 10^{19} \text{ W/cm}^2$ ,  $\lambda = 1 \mu\text{m}$ ) [2] hot-electron spectra vs kinetic energy  $\varepsilon_k$  for total initial electron number  $N_0 = 10^{20}$  and different initial electron velocities.

sponding to the second hot-electron peak is strongly dependent on the initial velocity. If we neglect the effect of initial motion on the quiver motion of the electrons, the second hot-electron peak will disappear. The effects of the moving directions of initial electrons on the hot-electron population are plotted in Fig. 2. One can also see that, unlike the first hot-electron peak, the energy of the second hot-electron peak is strongly dependent on the moving direction of the initial electrons.

Applying this theory to another experiment [9] where the solid target was irradiated by an 807-nm laser pulse at a focal intensity near  $5 \times 10^{18} \text{ W/cm}^2$ , one can find that the maxi-

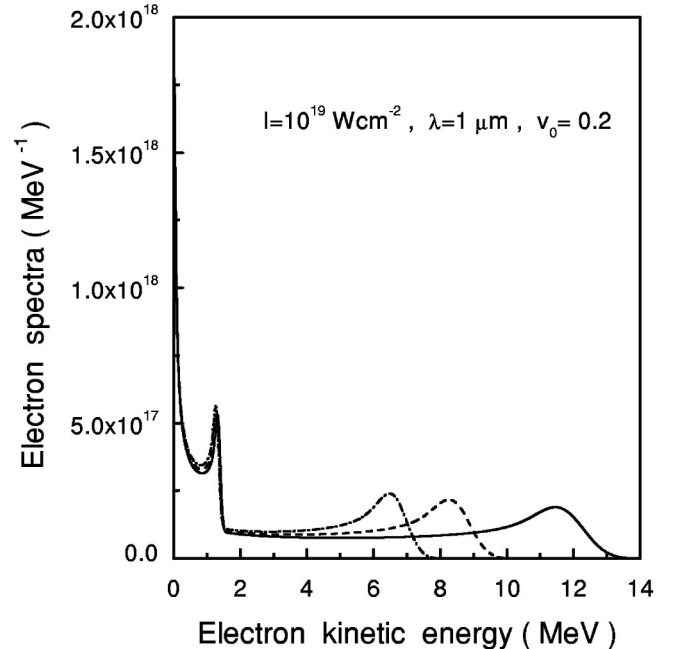


FIG. 2. Hot-electron spectra vs kinetic energies for total initial electron number  $N_0 = 10^{20}$  and different moving direction angles of initial electron:  $(\theta, \varphi) = \pi/2$  (solid line),  $\pi/3$  (dashed line), and  $\pi/4$  (dash-dotted line).

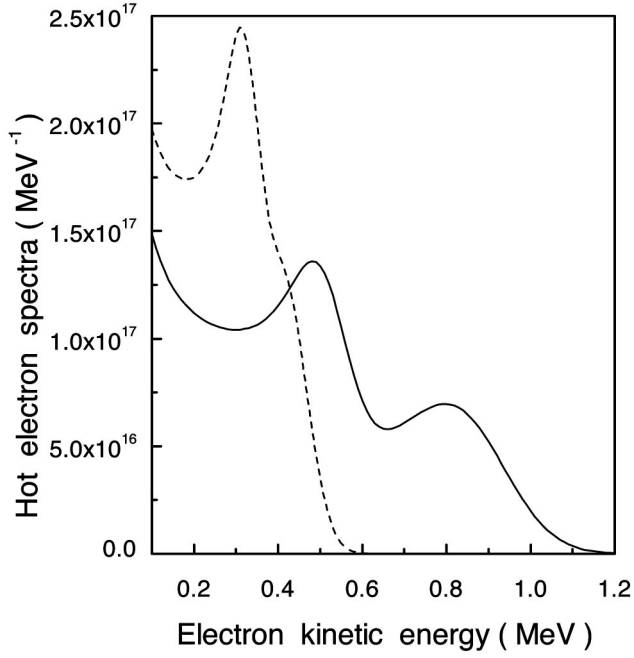


FIG. 3. Hot-electron spectra for 807 nm wavelength at intensities of  $3 \times 10^{18}$  and  $5 \times 10^{18}$  W/cm<sup>2</sup> with total initial electron number  $N_0 = 10^{20}$  and initial electron velocity  $v_0 = 0.3c$ .

imum energy of hot electrons is larger than 1 MeV (see solid line from Fig. 3), which may well explain the 1 MeV energy tail of hot electrons found in that experiment.

In order to further understand the acceleration of hot electrons, we give some discussions analytically. Assuming the electron energy in preplasmas as  $\varepsilon_0 = c(p_0^2 + m^2 c^2)^{1/2}$ , Eq. (4) becomes

$$\xi = \frac{(1/2)\gamma \cos \eta - \gamma_0 \cos \theta}{(1 + \gamma_0^2)^{1/2} - \gamma_0 \sin \theta \sin \varphi}, \quad (7)$$

where  $\gamma = v_E/c$ ,  $\gamma_0 = p_0/mc$ . For the longitudinal motion of initial electrons ( $\theta, \varphi = \pi/2$ ), factor  $\xi$  reaches its maximum value. If the LSP value and  $p_0$  are so large that  $\xi > 1$ , the direct longitudinal acceleration by the Lorentz force is larger than the direct transverse acceleration by the laser electric field. Therefore, we can find an important peak LSP threshold (taking  $\cos \eta = 1$ ) from the above calculations

$$(I\lambda^2)_{\text{th}} = 5.46 \times 10^{18} [(1 + \gamma_0^2)^{1/2} + \gamma_0 (\cos \theta - \sin \theta \sin \varphi)]^2 \quad (\text{W cm}^{-2} \mu\text{m}^2). \quad (8)$$

When the LSP value reaches this threshold, the acceleration effect in the longitudinal direction is equal to that in the transverse direction. Above the threshold the longitudinal acceleration becomes larger than the transverse acceleration

and the second hot-electron population peak appears accordingly. This implies that the second hot-electron population is mainly generated by the Lorentz force, while the first one is generated by the laser electric field. The generation of the second hot-electron peak and the corresponding energy are dependent on the preplasma conditions as well as on the LSP value of the main pulse. Within the incident plane of the laser beam,  $(I\lambda^2)_{\text{th}} \approx 5.46 \times 10^{18} \text{ W cm}^{-2} \mu\text{m}^2$  for initial electrons with lower energy ( $\gamma_0 \ll 1$ ),  $(I\lambda^2)_{\text{th}} \approx 5.46 \times 10^{18} (\sqrt{1 + \gamma_0^2} + \gamma_0)^2 \text{ W cm}^{-2} \mu\text{m}^2$  for initial electrons moving in the transverse direction, and  $(I\lambda^2)_{\text{th}} \approx 5.46 \times 10^{18} (\sqrt{1 + \gamma_0^2} - \gamma_0)^2 \text{ W cm}^{-2} \mu\text{m}^2$  for initial electrons moving in the longitudinal direction. It is apparent that the initial electrons moving in the longitudinal direction are easiest to accelerate in the interaction at very high laser intensities. In the nonrelativistic limit,  $\xi \ll 1$ , the longitudinal acceleration is much less than the transverse acceleration so that the longitudinal acceleration is negligible.

For a larger initial momentum of electrons moving in the laser propagating direction, the threshold is smaller and the acceleration effect due to the Lorentz force becomes stronger. This is evident either numerically or analytically. If we represent the longitudinal component in Eq. (2) with an effective laser strength parameter  $(I\lambda^2)_{\text{eff}}$ , Eq. (2) can be rewritten with a symmetric form

$$\mathbf{p}_E = -m v_E \mathbf{e}_x \cos \eta + m v'_E \mathbf{e}_z \cos \eta, \quad (9)$$

where the effective LSP value  $(I\lambda^2)_{\text{eff}} = I\lambda^2 / (\sqrt{1 + \gamma_0^2} - \gamma_0)^2$  is for the initial electrons moving longitudinally. It can be seen that, compared with the transverse component of  $\mathbf{p}_E$ , the LSP value in the longitudinal direction is enhanced if the energy of the initial electrons is large enough.

In summary, our calculations give a physical picture: (i) For lower LSP values and initial electron velocities, the acceleration effect of the Lorentz force on electrons is negligible when there is only one hot-electron population with lower energy. (ii) As the LSP value reaches and exceeds the threshold ( $\geq 5.5 \times 10^{18} \text{ W cm}^{-2} \mu\text{m}^2$ ) and the electrons in preplasmas are of higher velocities, the longitudinal acceleration produced by the Lorentz force leads to the second hot-electron population peak with higher energy, whereas the first hot-electron population is generated by laser electric field. (iii) Particularly for the prepulsed produced electrons moving in the axial direction, the LSP value can be enhanced by  $(\sqrt{1 + \gamma_0^2} - \gamma_0)^{-2}$  as well as be accelerated to several tens MeV energies by the Lorentz force of the laser magnetic field. These very hot electrons can travel through the critical density surface into targets due to the electrostatic screening effect, which may lead also to a change in the critical density surface.

This work was jointly supported by the National Natural Science Foundation of China (Grant No. 19854001) and the National Hi-Tech Inertial Confinement Fusion Committee.

- [1] G. Malka, J. Fuchs, F. Amiranoff, S. D. Baton, R. Gaillard, J. L. Miquel, H. Pepin, C. Rousseaux, G. Bonnaud, M. Busquet, and L. Lours, Phys. Rev. Lett. **79**, 2053 (1997).  
 [2] L. D. Landau and E. M. Lifshitz, *Classical Theory of Fields*, 4th ed. (Addison-Wesley, Reading, MA, 1975); J. J. Sander-

- son, Phys. Lett. **18**, 114 (1965); J. H. Eberly and A. Sleeper, Phys. Rev. **176**, 1570 (1968).  
 [3] B. N. Chichkov, S. A. Shumsky, and S. A. Uryupin, Phys. Rev. A **45**, 7475 (1992).  
 [4] A. Borisov *et al.*, Phys. Rev. A **45**, 5830 (1992); P. Monot

- et al.*, Phys. Rev. Lett. **74**, 2953 (1995); P. Young *et al.*, *ibid.* **75**, 1082 (1995); A. Chiron *et al.*, Phys. Plasmas **3**, 1373 (1996); M. Borghesi *et al.*, Phys. Rev. Lett. **78**, 879 (1997).
- [5] D. W. Forslund, J. M. Kindel, W. B. Mori, C. Joshi, and J. M. Dawson, Phys. Rev. Lett. **54**, 558 (1985).
- [6] T. C. Chiou, T. Katsouleas, and W. B. Mori, Phys. Plasmas **3**, 1700 (1996).
- [7] W. L. Kruer, *The Physics of Laser Plasma Interactions* (Addison-Wesley, Reading, MA, 1988).
- [8] A. Pukhov and J. Meyer-ter-Vehn, Phys. Rev. Lett. **76**, 3975 (1996).
- [9] J. D. Kmetec, C. L. Gordon, J. J. Macklin, B. E. Lemoff, G. S. Brown, and S. E. Harris, Phys. Rev. Lett. **32**, 1420 (1992).